J|A|C|S
ARTICLES
Published on Web 10/02/2004

Reactivity of Aqueous Fe(IV) in Hydride and Hydrogen Atom Transfer Reactions

Oleg Pestovsky and Andreja Bakac*

Contribution from the Ames Laboratory, Iowa State University of Science and Technology, Ames, Iowa 50011

Received July 16, 2004; E-mail: bakac@ameslab.gov

Abstract: Oxidation of cyclobutanol by aqueous Fe(IV) generates cyclobutanone in ~70% yield. In addition to this two-electron process, a smaller fraction of the reaction takes place by a one-electron process, believed to yield ring-opened products. A series of aliphatic alcohols, aldehydes, and ethers also react in parallel hydrogen atom and hydride transfer reactions, but acetone and acetonitrile react by hydrogen atom transfer only. Precise rate constants for each pathway for a number of substrates were obtained from a combination of detailed kinetics and product studies and kinetic simulations. Solvent kinetic isotope effect for the self-decay of Fe(IV), $k_{H_2O}/k_{D_2O} = 2.8$, is consistent with hydrogen atom abstraction from water.

Introduction

High-valent iron oxo complexes have attracted considerable attention in the context of catalytic C−H bond activation in both laboratory and biological oxidations. Attempts to unravel and mimic the chemistry of both heme and nonheme iron centers in enzyme active sites have focused on structures, mechanisms, and intermediates.[1−12] Mononuclear nonheme iron oxo complexes[13] are of particular interest for catalytic applications, but the successful synthesis and characterization of such compounds have been limited by their high reactivity and instability under ambient conditions.[14−16] Literature data on mechanistic aspects of C−H bond activation by iron oxo complexes, for example, the preference for 1-electron vs 2-electron mechanisms, are quite limited.[15,17] Such information could be especially useful in the design of catalytic systems utilizing O_2 and H_2O_2, since successful catalysis often requires two-electron steps.

Surprisingly, there is only a limited mechanistic information available for the simplest and one of the most reactive high-valent iron oxo complexes, aqueous Fe(IV), which can be conveniently generated from Fe_{aq}^{2+} and ozone[18,19] and has a lifetime of several seconds at room temperature in acidic aqueous solutions. Reactions with a limited number of organic substrates were reported to take place by an initial hydrogen atom transfer, but no product analyses were carried out to confirm this assignment which was based on the kinetics alone.[20] Another report provided kinetic evidence for a two-electron oxidation of substituted phenols via an Fe(IV)−substrate complex.[21]

Our own work on the chemistry of aqueous Cr(IV) has demonstrated quite the opposite trends in reactivity, that is, two-electron oxidation of alcohols and one-electron oxidation of phenols.[22,23] These unusual findings become even more intriguing in light of the thermodynamics of these reactions. The standard reduction potentials for the M_{aq}^{III}/M_{aq}^{II} couples are −0.41 V for chromium and 0.77 V for iron, demonstrating the thermodynamic preference for the formation of Cr_{aq}^{3+} (one-electron product) and Fe_{aq}^{2+} (two-electron product). Clearly, other factors determine the outcome of these reactions.

The one-electron potential for $Fe_{aq}^{IV/III}$ is not available. For the $Cr_{aq}^{IV/III}$ couple, only an estimate of ≥1.7 V exists. The reported chemistry of Fe_{aq}^{IV} suggests that the IV/III potential may be much greater than that for the $Cr_{aq}^{IV/III}$ couple, and the 1-e path, although less favorable, may still have a great driving force. Alternatively, the precise chemical environment may be

(1) Meunier, B.; Bernadou, J. *Struct. Bonding (Berlin)* **2000**, *97*, 1−35.
(2) Tshuva, E. Y.; Lippard, S. J. *Chem. Rev.* **2004**, *104*, 987−1011.
(3) Costas, M.; Mehn, M. P.; Jensen, M. P.; Que, L., Jr. *Chem. Rev.* **2004**, *104*, 939−986.
(4) Karlin, K. D. *Science* **1993**, *261*, 701−708.
(5) Merkx, M.; Kopp, D. A.; Sazinsky, M. H.; Blazyk, J. L.; Muller, J.; Lippard, S. J. *Angew. Chem., Int. Ed.* **2001**, *40*, 2782−2807.
(6) Ito, M.; Fujisawa, K.; Kitajima, N.; Moro-Oka, Y. *Catalysis by Metal Complexes* **1997**, *19 (Oxygenases and Model Systems)*, 345−376.
(7) Que, L., Jr.; Tolman, W. B. *Angew. Chem., Int. Ed.* **2002**, *41*, 1114−1137.
(8) Groves, J. T. *Proc. Natl. Acad. Sci. U.S.A.* **2003**, *100*, 3569−3574.
(9) Gray, H. B. *Proc. Natl. Acad. Sci. U.S.A.* **2003**, *100*, 3563−3568.
(10) De Montellano, P. R. O.; De Voss, J. J. *Nat. Prod. Rep.* **2002**, *19*, 477−493.
(11) Green, M. T.; Dawson, J. H.; Gray, H. B. *Science* **2004**, *304*, 1653−1656.
(12) Nam, W.; Park, S.-E.; Lim, I. K.; Lim, M. H.; Hong, J.; Kim, J. *J. Am. Chem. Soc.* **2003**, *125*, 14674−14675.
(13) Solomon, E. I.; Decker, A.; Lehnert, N. *Proc. Natl. Acad. Sci. U.S.A.* **2003**, *100*, 3589−3594.
(14) Grapperhaus, C. A.; Mienert, B.; Bill, E.; Weyhermueller, T.; Wieghardt, K. *Inorg. Chem.* **2000**, *39*, 5306−5317.
(15) Kaizer, J.; Klinker, E. J.; Oh, N. Y.; Rohde, J.-U.; Song, W. J.; Stubna, A.; Kim, J.; Muenck, E.; Nam, W.; Que, L., Jr. *J. Am. Chem. Soc.* **2004**, *126*, 472−473.
(16) Rohde, J.-U.; In, J.-H.; Lim, M. H.; Brennessel, W. W.; Bukowski, M. R.; Stubna, A.; Muenck, E.; Nam, W.; Que, L., Jr. *Science* **2003**, *299*, 1037−1039.
(17) Price, J. C.; Barr, E. W.; Glass, T. E.; Krebs, C.; Bollinger, J. M., Jr. *J. Am. Chem. Soc.* **2003**, *125*, 13008−13009.
(18) Loegager, T.; Holcman, J.; Sehested, K.; Pedersen, T. *Inorg. Chem.* **1992**, *31*, 3523−3529.
(19) Jacobsen, F.; Holcman, J.; Sehested, K. *Int. J. Chem. Kinet.* **1997**, *29*, 17−24.
(20) Jacobsen, F.; Holcman, J.; Sehested, K. *Int. J. Chem. Kinet.* **1998**, *30*, 215−221.
(21) Martire, D. O.; Caregnato, P.; Furlong, J.; Allegretti, P.; Gonzalez, M. C. *Int. J. Chem. Kinet.* **2002**, *34*, 488−494.
(22) Scott, S. L.; Bakac, A.; Espenson, J. H. *J. Am. Chem. Soc.* **1992**, *114*, 4205−4213.
(23) Bakac, A. *Prog. Inorg. Chem.* **1995**, *43*, 267−351.

different for the two metal(IV) aqua species. $Cr_{aq}(IV)$ is believed to be an oxoaqua species, $Cr_{aq}O^{2+}$, owing to the great oxophilicity of chromium. The iron(IV), on the other hand, has been suggested[20] to exist as a mixture of two hydrolytic forms, $Fe_{aq}(OH)_2^{2+}$ and $Fe_{aq}(OH)_3^{+}$, related by a pK_a of 2.0. The lack of an oxo group may make the hydrogen atom transfer a preferable path for iron provided such a path is thermodynamically allowed.

Here we report the results of a kinetic and mechanistic study of the oxidation of a number of organic substrates with aqueous Fe(IV). To simplify chemical equations, we will use the formula $Fe^{IV}O^{2+}$ to represent all forms of Fe(IV) in solution.

Experimental Section

Materials. Methanol, methanol-d_3, ethanol, 2-propanol, 2-propanol-d_1, -d_6, and -d_8, 2-butanol, benzyl alcohol, *para*-substituted benzyl alcohols, cyclobutanol, cyclobutanone, propionaldehyde, benzaldehyde, paraform, acetone, diethyl ether, THF, acetonitrile, acetonitrile-d_3, 1,10-phenanthroline, sodium acetate, hydrogen peroxide, chromium(III) perchlorate, iron(III) perchlorate, titanium(IV) oxysulfate, perchloric acid, and D_2O were of highest purity from commercial sources (Aldrich, Fisher, Cambridge Isotope Laboratories) and were used as received. Deionized water was obtained by passage of in-house distilled water through a Millipore Milli-Q water purification system.

Fe_{aq}^{2+} stock solutions were prepared by Zn/Hg reduction of 0.010 M Fe_{aq}^{3+} in 0.10 M $HClO_4$. The amount of residual Fe_{aq}^{3+} was determined by UV−vis spectrophotometry, ϵ_{240} (Fe_{aq}^{3+}) = 4160 M^{-1} cm^{-1}, and never exceeded 0.1% of initial Fe_{aq}^{2+}. Ozone was generated with an Ozonology L-100 apparatus. Aqueous solutions of ozone were prepared by continuous bubbling of ozone through 0.10 M $HClO_4$ for at least 30 min at room temperature. Such solutions, standardized spectrophotometrically, ϵ_{260} (O_3) = 3300 M^{-1} cm^{-1},[24] contained approximately 0.5 mM O_3. Titanium oxysulfate test (see below) showed no detectable quantities (<2 μM) of H_2O_2 in ozone stock solutions. $Cr_{aq}O^{2+}$ solutions were prepared as described previously[22] and contained approximately 50 μM $Cr_{aq}O^{2+}$ and 17 μM $Cr_{aq}OO^{2+}$. Stock solutions of formaldehyde were prepared by dissolving a known amount of paraform in warm 1.0 M $HClO_4$.

Kinetics All the kinetics studies were carried out at 25 ± 0.1 °C in 0.10 M aqueous $HClO_4$, unless stated otherwise. For fast reactions, an OLIS RSM-1000 stopped-flow apparatus was used. The reaction between $Fe^{IV}O^{2+}$ and Fe_{aq}^{2+} was studied at high [Fe_{aq}^{2+}] to ensure that all the $Fe^{IV}O^{2+}$ was generated in the first few milliseconds, which were not used in the kinetic fitting. In the experiments on substrate oxidation by $Fe^{IV}O^{2+}$, one stopped-flow syringe contained the ozone solution, and the other, a mixture of Fe_{aq}^{2+} and substrate. After mixing, the typical concentration of ozone was 0.25 mM, and that of Fe_{aq}^{2+}, 0.10 mM. Under these conditions, $Fe^{IV}O^{2+}$ was generated in the first few milliseconds. The small, controlled excess of ozone was necessary to scavenge any Fe_{aq}^{2+} produced in 2-e steps (see Results) and, thus, prevent the Fe_{aq}^{2+}/ $Fe^{IV}O^{2+}$ reaction and the associated absorbance changes caused in large part by the formation and decay of dimeric Fe(III). The data, obtained by rapid scanning (Δt = 1 ms) in the 265−392 nm spectral range, were analyzed with the use of OLIS Global-Works v2.0.190 software. The rate constants were obtained as averages of at least three experiments. Slower reactions were monitored with a Shimadzu 3101 PC spectrophotometer. Kinetics of the reaction between Fe_{aq}^{2+} and H_2O_2 in the presence of alcohols were studied by monitoring the increase in Fe_{aq}^{3+} concentration at 240 nm.

The analyses of kinetic data were performed with Kaleidagraph v3.51 for PC software. Kinetic simulations were carried out with Kinsim v4.0 software.

The kinetic isotope effect for the self-decay of $Fe^{IV}O^{2+}$ was calculated from the expression

$$k_H/k_D = \frac{k_{2H}}{k_{2D}} \frac{(100 - \%H)}{\{100 - (\%H \times k_{2H}/k_{2D})\}}$$

where k_{2H} and k_{2D} are the respective rate constants for reaction 2 (see later) in H_2O and D_2O.

Conductivity measurements were carried out at 26.5 °C with the use of a TDI model VI stopped-flow apparatus equipped with a custom-built TDI conductivity cell and ranging amplifier.[25] The signal output was amplified and offset to bring it into the dynamic range of the instrument. An average of three independent runs was used to determine the rate constants and the associated conductivity changes. Ultimately, these data yielded the change in proton concentration during the run and the overall charge on the $Fe^{IV}O^{2+}$ ion.

Product Analysis. For UV-transparent substrates (methanol, ethanol, 2-propanol, THF, formaldehyde, and cyclobutanol), the yields of Fe_{aq}^{2+} were obtained as a difference between the known initial concentration of Fe_{aq}^{2+} and the amount of Fe_{aq}^{3+} determined by direct conventional spectrophotometry at 240 nm immediately following the manual mixing of the reagents. For benzyl alcohol, *p*-CF_3-benzyl alcohol, acetone, and acetonitrile, the reaction mixture was combined with 0.17 mM phenanthroline (added as acetonitrile solution, giving a final acetonitrile content of 3.9%) and 0.14 M sodium acetate. The absorbance reading was taken at 510 nm, where $Fe(phen)_3^{2+}$ has an extinction coefficient of 1.14 × 10^4 M^{-1} cm^{-1}. This method proved to be less precise than the direct spectrophotometry, because some Fe_{aq}^{2+} (5−10 μM) was consumed in the reaction with H_2O_2 during the analysis.

The yields of H_2O_2 were determined by adding 20 μL of $TiOSO_4$ reagent (1.42 M in 15% H_2SO_4) to a 3-mL sample solution. The titanium peroxo complex, ϵ_{408} = 723 M^{-1} cm^{-1}, was formed immediately and quantitatively. However, in experiments containing both Fe_{aq}^{2+} and H_2O_2 in the spent solution (see Results), the initially formed titanium peroxo complex decayed rapidly (minutes or less).[26] The yields of H_2O_2 were obtained by extrapolation to zero time.

As a double check for solutions containing both H_2O_2 and Fe_{aq}^{2+}, the peroxide yields were also calculated from the initial rates of the Fe_{aq}^{2+}/H_2O_2 reaction and the mechanism in Scheme 1, where k_F is the rate constant for the Fenton reaction.

According to the scheme, the hydrolysis of hydroxyalkyl hydroperoxides regenerates H_2O_2, which thus becomes a catalyst for the co-oxidation of Fe_{aq}^{2+} and alcohols by O_2. Pseudo-first-order kinetics with respect to [Fe_{aq}^{2+}] should be obeyed when sufficient amounts of O_2 are present. A more complex kinetic behavior results when hydrogen peroxide is consumed in side reactions or is not regenerated from a particular peroxide. Any complications resulting from changing [H_2O_2] were avoided by use of initial rates. The method was checked with authentic reagents for the case Fe_{aq}^{2+} (43 μM)/H_2O_2 (30−50 μM)/cyclobutanol (0.102 M). As expected, the initial rates, V_i, obeyed the rate law, $V_i = 2 \times k_F \times [H_2O_2] \times [Fe_{aq}^{2+}]$, where k_F = 58 M^{-1} s^{-1}, the known rate constant for the Fe_{aq}^{2+}/H_2O_2 reaction.[27] The amount of hydrogen peroxide produced in the reactions between $Fe^{IV}O^{2+}$ and substrates was calculated as $[H_2O_2] = V_i/(2k_F \times [Fe_{aq}^{2+}])$.

^1H NMR spectra were recorded with a Varian VXR-400 spectrometer at room temperature.

Results

$Fe^{IV}O^{2+}$ Formation and Decay. Literature data already exist for both the Fe_{aq}^{2+}/O_3 reaction and the decay of $Fe^{IV}O^{2+}$ in acidic aqueous solutions.[18−20] Because the reaction scheme with added substrates is complex (see later), precise kinetic data for reactions 1 and 2 under our exact experimental conditions were

(24) Hart, E. J.; Sehested, K.; Holcman, J. *Anal. Chem.* **1983**, *55*, 46−49.

(25) Knipe, A. C.; McLean, D.; Tranter, R. L. *J. Phys. E: Sci. Instrum.* **1974**, *7*, 586−590.

(26) This rapid reaction between $TiO(SO_4)/H_2SO_4$ and Fe_{aq}^{2+} stands in contrast to the very slow reaction reported in the perchlorate medium.[53]

(27) Wang, W. D.; Bakac, A.; Espenson, J. H. *Inorg. Chem.* **1993**, *32*, 2005−2009.

Scheme 1

$$Fe_{aq}^{2+} + H_2O_2 \xrightarrow{k_F} Fe_{aq}^{3+} + {}^{\bullet}OH$$

$$^{\bullet}OH + R_2CHOH \longrightarrow H_2O + R_2{}^{\bullet}COH$$

$$R_2{}^{\bullet}COH + O_2 \longrightarrow R_2C(OH)\text{-}OO^{\bullet}$$

$$R_2C(OH)\text{-}OO^{\bullet} + Fe_{aq}^{2+} \xrightarrow{H^+} Fe_{aq}^{3+} + R_2C(OH)\text{-}OOH$$

$$R_2C(OH)\text{-}OOH \longrightarrow R_2C{=}O + H_2O_2$$

required. The results of our extensive and detailed kinetics experiments agreed well with those reported in the literature and are briefly summarized below.

The reaction between 0.010−0.020 mM Fe_{aq}^{2+} and 0.10−0.20 mM O_3 followed pseudo-first-order kinetics with an isosbestic point at 291 nm, eq 1.

$$Fe_{aq}^{2+} + O_3 \rightarrow Fe^{IV}O^{2+} + O_2 \qquad (1)$$

The disappearance of ozone dominated the absorbance changes below 291 nm, and the formation of $Fe^{IV}O^{2+}$ was observed above 291 nm, Figure S1 (Supporting Information). Global fitting of the kinetic data to the {A → B} model afforded a series of pseudo-first-order rate constants, which varied linearly with [O_3] and yielded $k_1 = (8.30 \pm 0.10) \times 10^5$ M^{-1} s^{-1}. At longer times, an approximately exponential decay of $Fe^{IV}O^{2+}$ was detected above 300 nm, $k_{2H} = 0.10$ s^{-1} at pH 1.0, eq 2. Solutions of $Fe^{IV}O^{2+}$ in D_2O (7.6% H) at pD 1.0 were somewhat more stable, with a decay rate constant $k_{2D} = 0.040$ s^{-1}, yielding a solvent kinetic isotope effect of 2.85.

$$Fe^{IV}O^{2+} (+ H^+) \rightarrow Fe_{aq}^{3+} + {}^1/_4\, O_2 + {}^1/_2\, H_2O \qquad (2)$$

In experiments using Fe_{aq}^{2+} (0.460−0.720 mM) in excess over O_3 (0.023 mM), the disappearance of $Fe^{IV}O^{2+}$ was accompanied by hydrolysis of $Fe_{aq}(OH)_2Fe_{aq}^{4+}$,[19] eqs 3 and 4.

$$Fe^{IV}O^{2+} + Fe_{aq}^{2+} \rightarrow 2\, Fe_{aq}^{3+}/Fe_{aq}(OH)_2Fe_{aq}^{4+} \qquad (3)$$

$$Fe_{aq}(OH)_2Fe_{aq}^{4+} + (2\, H^+) \rightarrow 2\, Fe_{aq}^{3+} + 2\, H_2O \qquad (4)$$

A global fit to the {A → B → C} model afforded $k_3 = (4.33 \pm 0.01) \times 10^4$ M^{-1} s^{-1} and $k_4 = 0.79$ s^{-1} (in 0.10 M $HClO_4$), Figure S2.

A cursory study of the oxidation of several substrates with O_3 was carried out by monitoring the disappearance of O_3 at 260 nm. These single-point experiments utilized a large excess of the substrate (1−30 mM) over O_3 (0.2 mM). The reactions were assumed to be first-order in each reagent, and second-order rate constants were obtained by dividing the measured pseudo-first-order rate constants by the substrate concentrations. The rate constants (ethanol, 0.59 M^{-1} s^{-1}; propionaldehyde, 5.9 M^{-1} s^{-1}; benzaldehyde, 9.7 M^{-1} s^{-1}; cyclobutanol, 2.1 M^{-1} s^{-1}) were several orders of magnitude smaller than those for the reactions of these substrates with $Fe^{IV}O^{2+}$. This rules out any interference from ozone in the $Fe^{IV}O^{2+}$/substrate reactions under any conditions in this work.

A series of stopped-flow conductivity measurements was carried out to determine the number of proton equivalents consumed during the $Fe^{IV}O^{2+}$ decay. The top trace in Figure 1 shows the decay of 0.18 mM $Fe^{IV}O^{2+}$ (obtained by mixing 0.20 mM Fe_{aq}^{2+} and 0.25 mM O_3). The control reaction between

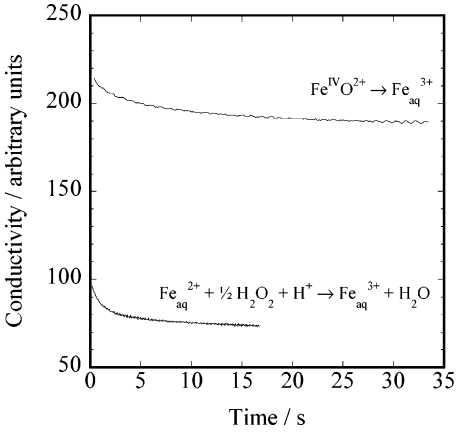

Figure 1. Conductivity changes observed in the reaction between 0.20 mM Fe_{aq}^{2+} and 9.7 mM H_2O_2 (bottom) and in self-decay of 0.18 mM $Fe^{IV}O^{2+}$ [obtained by mixing 0.20 mM Fe_{aq}^{2+} and 0.25 mM O_3] (top) in 0.10 M $HClO_4$ at 25 °C.

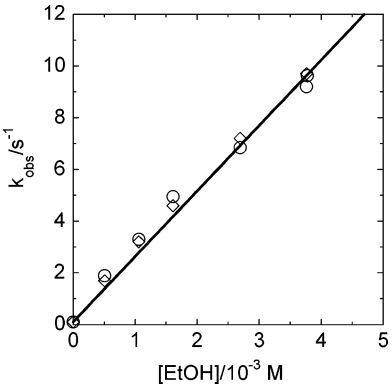

Figure 2. Plot of pseudo-first-order rate constants (circles) against the concentration of ethanol for the reaction with $Fe^{IV}O^{2+}$. Solid line represents the fit to eq 6 for $k_{obs} > 4$ s^{-1}. Simulated data (see text) are shown as diamonds. Conditions: [Fe_{aq}^{2+}] = 0.10 mM, [O_3] = 0.25 mM, [$HClO_4$] = 0.10 M, [O_2] = 0.4 mM, 25 °C.

0.20 mM Fe_{aq}^{2+} and 9.7 mM H_2O_2 yielded the bottom trace in Figure 1. This reaction is known to take place as in eq 5 and to consume 1 equiv of H^+ for each Fe_{aq}^{2+} oxidized. The nearly identical amplitudes cleanly demonstrate the same overall consumption of proton equivalents in the two experiments. Since both reactions 2 and 5 yield Fe_{aq}^{3+} as a product, and they consume the same number of hydrogen ions, the reactants must also have the same overall charge. We conclude that Fe(IV) in 0.10 M $HClO_4$ bears a 2+ charge.

$$Fe_{aq}^{2+} + 0.5\, H_2O_2 + H^+ \rightarrow Fe_{aq}^{3+} + H_2O \qquad (5)$$

Kinetics of Substrate Oxidations by $Fe^{IV}O^{2+}$. The reaction between $Fe^{IV}O^{2+}$ and ethanol utilized a large excess of ethanol, 0.50−3.8 mM. The pseudo-first-order disappearance of $Fe^{IV}O^{2+}$ was observed above 300 nm in <1 s, followed by small absorbance changes (<5% of the total) in approximately 10−20 s. We attribute the slower process to the combination of the ethanol/O_3 reaction and hydrolysis of $Fe_{aq}(OH)_2Fe_{aq}^{4+}$. Global fitting of the data to the {A → B → C} model produced pseudo-first-order rate constants shown as a function of [EtOH] in Figure 2. The dependence is described by eq 6, where k_{2H} (0.10 s^{-1}) is the rate constant for the $Fe^{IV}O^{2+}$ decay in the absence of ethanol. The slope, calculated only from the rate constants ≥ 4 s^{-1} (see Discussion) yielded $k_S = (2.51 \pm 0.08) \times 10^3$

Table 1. Summary of Observed Second-Order Rate Constants k_S for the Oxidations with $Fe^{IV}O^{2+}$ [a]

substrate	k_S/ $M^{-1}\,s^{-1}$ [b,c]	substrate	k_S/ $M^{-1}\,s^{-1}$ [b,c]
CH_3OH	5.72×10^2	p-$CH_3-C_6H_4-CH_2OH$	1.50×10^4
CH_3OD [d]	5.72×10^2	p-$CH_3O-C_6H_4-CH_2OH$	1.59×10^4
CD_3OH	1.26×10^2	cyclobutanol	3.13×10^3
C_2H_5OH	2.51×10^3	CH_2O	7.72×10^2
	2.50×10^3 [e]		4.00×10^2 [e]
$(CH_3)_2CHOH$	3.22×10^3	C_2H_5CHO	2.85×10^4
$(CD_3)_2CHOH$	3.07×10^3	C_6H_5CHO	2.07×10^4
$(CH_3)_2CDOH$	7.00×10^2	Et_2O	4.74×10^3
$(CD_3)_2CDOH$	6.60×10^2	THF	7.46×10^3
$CH_3CH(OH)CH_2CH_3$	4.04×10^3	HCOOH	1.60×10^2 [e]
$(CH_3)_3COH$	6.0×10^1	$HCOO^-$	3×10^5 [e]
p-$CF_3-C_6H_4-CH_2OH$	1.00×10^4	CH_3COOH	3.1[e]
p-$Br-C_6H_4-CH_2OH$	1.41×10^4	C_6H_5COOH	80[e]
$C_6H_5-CH_2OH$	1.42×10^4	CH_3COCH_3 [f]	31.5
			16[e]
		CH_3CN	4.12

[a] Conditions: $[Fe_{aq}^{2+}] = 0.10$ mM, $[O_3] = 0.25$ mM, $[HClO_4] = 0.10$ M, $[O_2] = 0.4$ mM, 25 °C. [b] Obtained from a global fit in the range 265−392 nm. [c] Uncertainty: ±10%. [d] In D_2O. [e] Reference 20. [f] Determined at 320 nm, [acetone] = 4.5−9.0 mM.

$M^{-1}\,s^{-1}$. Although the uncertainty for k_S obtained from the fit is ±3%, the complexity of the system and the need to remove the data at low [EtOH] suggest a more realistic error of ±10%.

$$k_{obs} = k_{2H} + k_S \times [EtOH] \qquad (6)$$

Similar methodology was also used to determine kinetic parameters for the rest of the substrates in Table 1. The kinetic data and results of the global fit analysis for the oxidation of propionaldehyde are shown in Figures S3 and S4 in the Supporting Information.

Products and Stoichiometry. For alcohols, aldehydes, and ethers as substrates, a slow reaction was detected by conventional UV−vis spectrophotometry after all the $Fe^{IV}O^{2+}$ had been consumed. The absorbance of the mixture initially having 0.130 mM O_3, 0.125 mM Fe_{aq}^{2+}, and 0.10 M 2-propanol was followed at 240 nm. The initial absorbance reading, taken immediately after the O_3 injection, was consistent with only partial formation of Fe_{aq}^{3+} (~63%). Note that, at such high substrate concentration, the reaction between 2-propanol and $Fe^{IV}O^{2+}$ is completed in milliseconds. All the missing Fe_{aq}^{3+} was formed in a subsequent slow biexponential step taking approximately 3000 s, Figure S5. It is clear that the theoretical 1:1 stoichiometry for the reaction between Fe_{aq}^{2+} and O_3 is not obeyed in the presence of organic substrates.

The immediate stoichiometry in the Fe_{aq}^{2+}/O_3/substrate system was determined by making multiple injections of O_3 stock solutions into a mixture of 0.125 mM Fe_{aq}^{2+} and 0.56 M methanol or 0.126 M ethanol and taking absorbance readings at 240 nm. The direction of the absorbance change on the 3000 s time scale was then used to determine which reagent was in excess: an absorbance rise signaled excess Fe_{aq}^{2+} (being slowly oxidized to Fe_{aq}^{3+}), while an absorbance decrease indicated excess O_3 (slowly going away). Complete consumption of both Fe_{aq}^{2+} and O_3 occurred at 1:2.4 (methanol) and 1:1.7 (ethanol) ratios of Fe_{aq}^{2+} to ozone. The resulting solutions, containing no leftover Fe_{aq}^{2+} or ozone, were also analyzed for H_2O_2 with titanium oxysulfate. The amounts found were 47 and 46 μM for experiments with methanol and ethanol, respectively. Thus the Fe_{aq}^{2+}/H_2O_2 reaction is clearly the one responsible for the slow formation of additional Fe_{aq}^{3+} in the above experiments.

Table 2. Final Concentrations of Fe_{aq}^{2+} and H_2O_2 in Fe_{aq}^{2+}/O_3/Substrate Reactions[a]

substrate	$[Fe_{aq}^{2+}]/\mu M$	$[H_2O_2]/\mu M$
methanol	59	29,[f] 26[g]
	45[b]	
	48[b,c]	
	42[b,d]	
	46[b,e]	
ethanol	40	34,[f] 33[g]
2-propanol	46	29,[f] 36[g]
THF	9	49[f]
CH_2O [h]	55	29[f]
cyclobutanol	42	46,[f] 35[g]
$PhCH_2OH$	14[b]	*i*
p-$CF_3-Ph-CH_2OH$	12[b]	*i*
CH_3CN	*b, j*	*i*
CH_3COCH_3	*b, j*	*i*

[a] Conditions: 0.125 mM Fe_{aq}^{2+}, 0.130 mM O_3, 45−560 mM substrate, 0.10 M $HClO_4$, 0.4 mM O_2, 25 °C. [b] By phenanthroline test. [c] In 0.026 M $HClO_4$. [d] In 0.195 M $HClO_4$. [e] In 93% D_2O. [f] Initial rates method; see Experimental Section. [g] Titanium oxysulfate method; see Experimental Section. [h] In 0.156 M $HClO_4$. [i] Not determined. [j] Below detection limit.

Next, a series of experiments were carried out to quantitate the yields of Fe_{aq}^{2+} and H_2O_2 in the reaction of $Fe^{IV}O^{2+}$ with a number of substrates at nearly equimolar amounts of Fe_{aq}^{2+} (0.125 mM) and O_3 (0.130 mM). The substrates used were, in separate experiments, 0.560 M methanol, 0.126 M ethanol, 0.0452 M THF, 0.416 M formaldehyde, 0.0225 M benzyl alcohol, 0.0162 M p-CF_3-benzyl alcohol, 1.28 M acetonitrile, 0.908 M acetone, or 0.102 M cyclobutanol. These particular concentrations were chosen to make the rate of $Fe^{IV}O^{2+}$ consumption identical to that in the experiment with 2-propanol described above. The amounts of Fe_{aq}^{2+} and H_2O_2, determined as described in the Experimental Section, are shown in Table 2.

The yields of Fe_{aq}^{2+} were largely unaffected by changing the acid concentration in the range 0.026−0.195 M $HClO_4$ or by replacing H_2O with D_2O as solvent, Table 2.

The products of the reaction between cyclobutanol (4.16 mM in D_2O containing 3.2% H and 3.2% CD_3CN) and $Fe^{IV}O^{2+}$ (generated from 0.20 mM Fe_{aq}^{2+} and 0.20 mM O_3) were examined by ^1H NMR spectrometry. The main product was cyclobutanone, 0.129 mM, as determined by its characteristic triplet at 3.02 ppm, Figure 3. Resonances from other possible products could not be observed in the presence of residual H_2O and unreacted cyclobutanol.

In a parallel experiment, cyclobutanol was allowed to react with 50 μM $Cr_{aq}O^{2+}$. In this case, no cyclobutanone was detected. This result is consistent with our earlier work[22] in which the $Cr_{aq}O^{2+}$/cyclobutanol reaction failed to generate Cr_{aq}^{2+} and was concluded to take place by a one-electron, hydrogen atom transfer mechanism.

Discussion

The oxidation of cyclobutanol to cyclobutanone by $Fe^{IV}O^{2+}$ is a straightforward demonstration of a two-electron process. Literature precedents on the subject are clear. Only a single-step, 2-e process will leave the ring intact while oxidizing the alcohol to the ketone.[28−32] We are not aware of any reports on

(28) Rocek, J.; Radkowsky, A. E. *J. Am. Chem. Soc.* **1973**, *95*, 7123−7132.
(29) Rocek, J.; Radkowsky, A. E. *J. Org. Chem.* **1973**, *38*, 89−94.

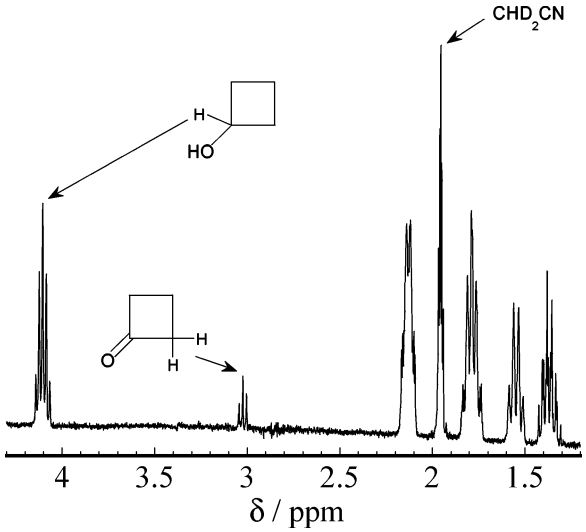

Figure 3. ^{1}H NMR spectrum of products generated from cyclobutanol (4.16 mM) and $Fe^{IV}O^{2+}$ (0.20 mM Fe_{aq}^{2+} + 0.20 mM O_3) in D_2O (0.10 M $DClO_4$, 3.2% H, 3.2% CD_3CN), at 25 °C and 0.4 mM O_2.

Scheme 2

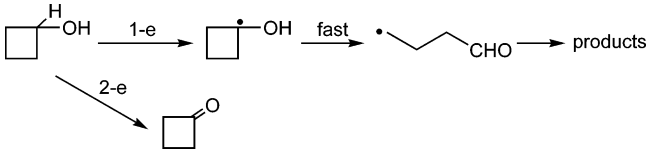

the ring-opening kinetics, but the sequence of 1-e steps appears to have produced ring-opened products in every case without exception,[33−35] Scheme 2. On this basis we conclude that the $Fe^{IV}O^{2+}$/cyclobutanol reaction proceeds mostly (∼70%) by a 2-e path, as judged by cyclobutanone yield.

Organic oxidation products for the rest of the substrates in Table 1 are not mechanism-sensitive. Both 1-e and 2-e oxidations produce aldehydes or ketones from the alcohols, carboxylic acids from aldehydes, and so on. The stoichiometric information embedded in inorganic products, on the other hand, allowed us to distinguish between 1-e and 2-e paths and, in combination with kinetic simulations, to quantify the proportions of each. Specifically, hydrogen peroxide and organic peroxides result from one-electron reactions involving radicals. The formation of Fe_{aq}^{2+} in the presence of high concentrations of O_2 and O_3, or the corollary, the overall $[O_3]/[Fe_{aq}^{2+}]$ stoichiometric ratio exceeding 1.0 in the presence of alcohols, aldehydes, and ethers, is indicative of a 2-e path. Importantly, this result cannot be explained by any other known chemistry, such as, for example, the consumption of O_3 by hydroxyalkyl radicals, despite the rate constants for reaction 7 exceeding 10^9 M^{-1} s^{-1}.[36] In the presence of (typically) 0.4 mM O_2, which also reacts rapidly with carbon-centered radicals,[37] only a negligible fraction of $R^•$ will react with the small amounts of ozone present. Similarly, the direct reaction between O_3 and the organic substrates is

Scheme 3

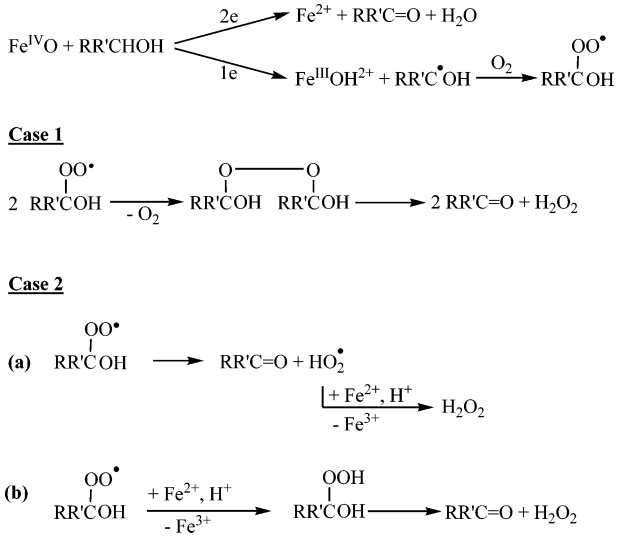

several orders of magnitude slower than any competing step, leaving the Fe_{aq}^{2+}/O_3 reaction as the only realistic ozone-consuming step. This reasoning was confirmed by kinetic simulations described below.

$$R^• + O_3 \rightarrow RO^• + O_2 \qquad (7)$$

Our general working mechanism is shown in Scheme 3. The initial branching between 1-electron and 2-electron paths determines the ratio of products, for instance, ring-opened products and Fe_{aq}^{3+} vs cyclobutanone and Fe_{aq}^{2+} in the cyclobutanol reaction. The radicals are scavenged by O_2 to give hydroxyalkyl peroxyl radicals. Those derived from methanol and ethanol disproportionate rapidly[38] ($k > 10^8$ M^{-1} s^{-1})[39,40] and give half an equivalent of hydroxyalkyl peroxide per radical, as in Case 1 of Scheme 3. Other hydroxyalkyl peroxyl radicals either eliminate $HO_2^•/O_2^{•-}$ (formaldehyde, 2-propanol),[41,42] Case 2a, or react directly with Fe_{aq}^{2+},[43] Case 2b. As a result, 1 equiv of Fe_{aq}^{2+} is oxidized to Fe_{aq}^{3+}, and 1 equiv of an organic hydroxyalkyl hydroperoxide or hydrogen peroxide is generated. Although hydroxyalkyl peroxides and hydroperoxides have been reported to hydrolyze rather slowly in slightly acidic or neutral solutions,[44,45] acid catalysis must be fast under our conditions to produce free H_2O_2.[46] The latter was identified unequivocally by the titanium(IV) oxysulfate test, which is known to be

(30) Mucientes, A. E.; Gabaldon, R. E.; Poblete, F. J.; Villarreal, S. *J. Phys. Org. Chem.* **2004**, *17*, 236−240.
(31) Wang, Z.; Chandler, W. D.; Lee, D. G. *Can. J. Chem.* **1998**, *76*, 919−928.
(32) Wiberg, K. B.; Mukherjee, S. K. *J. Am. Chem. Soc.* **1974**, *96*, 6647−6651.
(33) Meyer, K.; Rocek, J. *J. Am. Chem. Soc.* **1972**, *94*, 1209−1201.
(34) Rocek, J.; Radkowsky, A. E. *J. Am. Chem. Soc.* **1968**, *90*, 2986−2988.
(35) Lee, D. G.; Chen, T. *J. Org. Chem.* **1991**, *56*, 5341−5345.
(36) Sehested, K.; Holcman, J.; Bjergbakke, E.; Hart, E. J. *J. Phys. Chem.* **1987**, *91*, 2359−2361.
(37) Neta, P.; Grodkowski, J.; Ross, A. B. *J. Phys. Chem. Ref. Data* **1996**, *25*, 709−1050.
(38) Howard, J. A. In *Peroxyl Radicals*; Alfassi, Z. B., Ed.; Wiley: Chichester, 1997; pp 283−334.
(39) Huie, R. E.; Clifton, C. L. *Chem. Phys. Lett.* **1993**, *205*, 163−167.
(40) Bothe, E.; Schuchmann, M. N.; Schulte-Frohlinde, D.; Von Sonntag, C. *Z. Naturforsch., Teil B* **1983**, *38B*, 212−219.
(41) Bothe, E.; Behrens, G.; Schulte-Frohlinde, D. *Z. Naturforsch., B: Anorg. Chem., Org Chem.* **1977**, *32B*, 886−889.
(42) Bothe, E.; Schulte-Frohlinde, D. *Z. Naturforsch., B: Anorg. Chem., Org Chem.* **1980**, *35B*, 1035−1039.
(43) Mansano-Weiss, C.; Cohen, H.; Meyerstein, D. *J. Inorg. Biochem.* **2002**, *91*, 199−204.
(44) Dowideit, P.; von Sonntag, C. *Environ. Sci. Technol.* **1998**, *32*, 1112−1119.
(45) Zhou, X.; Lee, Y. N. *J. Phys. Chem.* **1992**, *96*, 265−272.
(46) This was confirmed for hydroxymethyl hydroperoxide prepared by equilibrating 0.10 M H_2O_2 and 0.46 M formaldehyde, $H_2O_2 + CH_2O \rightleftarrows HOOCH_2OH$. The equilibrated solution was diluted 300-fold in a spectrophotometric cell, $TiO(SO_4)$ was injected, and the absorbance increase was monitored at 408 nm. The rapid initial jump, corresponding to free H_2O_2, was followed by a slower absorbance increase, which we interpret as the hydrolysis of the hydroperoxide, pulled to completion by $H_2O_2/TiO(SO_4)$ reaction. The rate constant for H_2O_2 dissociation in 0.10 M $HClO_4$/0.01 M H_2SO_4 was 0.013 s^{-1}, 2 orders of magnitude larger than the reported rate constant at pH 4 (ref 45).

Scheme 4

(s1) $Fe_{aq}^{2+} + O_3 \rightarrow Fe^{IV}O^{2+} + O_2$

(s2) $Fe_{aq}^{2+} + Fe^{IV}O^{2+} (+ 2H^+) \rightarrow 2\ Fe_{aq}^{3+}$

(s3) $Fe^{IV}O^{2+} (+ H^+) \rightarrow Fe_{aq}^{3+} + OH^{\bullet}$

(s4) $Fe^{IV}O^{2+} + OH^{\bullet} (+ H^+) \rightarrow Fe_{aq}^{3+} + H_2O_2$

(s5) $Fe^{IV}O^{2+} + H_2O_2 (+ H^+) \rightarrow Fe_{aq}^{3+} + HO_2^{\bullet}$

(s6) $Fe^{IV}O^{2+} + HO_2^{\bullet} (+ H^+) \rightarrow Fe_{aq}^{3+} + O_2$

(s7) $Fe^{IV}O^{2+} + RCH_2OH (+ H^+) \rightarrow Fe_{aq}^{3+} + RC^{\bullet}H(OH)$

(s8) $Fe^{IV}O^{2+} + RCH_2OH \rightarrow Fe_{aq}^{2+} + RCHO$

(s9) $RC^{\bullet}H(OH) + O_3 \rightarrow RCH(OH)O^{\bullet} + O_2$

(s10) $RC^{\bullet}H(OH) + Fe_{aq}^{3+} \rightarrow RCHO + Fe_{aq}^{2+} + H^+$

(s11) $RC^{\bullet}H(OH) + O_2 \rightarrow RCH(OH)OO^{\bullet}$

(s12) $RCH(OH)O^{\bullet} + RCH_2OH \rightarrow RCHO + RC^{\bullet}H(OH)$

(s13) $OH^{\bullet} + RCH_2OH \rightarrow RC^{\bullet}H(OH) + H_2O$

(s14) $RCH(OH)OO^{\bullet} + Fe_{aq}^{2+} (+ H^+) \rightarrow RCHO + H_2O_2 + Fe_{aq}^{3+}$

(s15) $RCH(OH)OO^{\bullet} \rightarrow RCHO + HO_2^{\bullet}$

(s16) $HO_2^{\bullet} + Fe_{aq}^{2+} (+ H^+) \rightarrow H_2O_2 + Fe_{aq}^{3+}$

(s17) $2\ HO_2^{\bullet} \rightarrow H_2O_2 + O_2$

(s18) $2\ RCH(OH)OO^{\bullet} \rightarrow 2\ RCHO + O_2 + H_2O_2$

(s19) $RCH(OH)O^{\bullet} + Fe_{aq}^{2+} (+ H^+) \rightarrow RCHO + Fe_{aq}^{3+} + H_2O$

insensitive to organic peroxides and hydroperoxides.[47] The reasonably good agreement between the results obtained by the titanium method and the less peroxide-specific initial rate method (Table 2) rules out the presence of significant amounts of other peroxo species, which would increase the rate of disappearance of Fe_{aq}^{2+} and give a larger calculated concentration of H_2O_2. The method is however not precise enough to rule out completely the presence of small amounts of hydroperoxides.

The reactions used in kinetic simulations are summarized in Scheme 4 and Table 3. Data are not available for the ring-opened cyclobutanol-derived (alkyl) radical. The rate constants shown are those for *n*-propyl and *n*-butyl radicals, which are much less reactive than the hydroxyalkyl radicals in reactions with Fe_{aq}^{3+} (reaction s10). Also, the dissociation of $HO_2^{\bullet}$ (reaction s15) from the alkylperoxyl radicals is slower than for hydroxyalkylperoxyl radicals. For reaction s14, the rate constant of $1.5 \times 10^6\ M^{-1}\ s^{-1}$ was chosen as the best value from a large number of similar rate constants.[43,48] The nearly constant k_{s14} for various peroxyl radicals represents the substitution limit at the Fe(II) center.

The simulations were carried out for each substrate by adjusting the rate constants for one-electron and two-electron processes until both the calculated pseudo-first-order rate constants for the disappearance of $Fe^{IV}O^{2+}$ and the yields of Fe_{aq}^{2+} matched the experimental values to within experimental errors.

Table 3. Simulation Rate Constants for Scheme 4[a]

reaction no.	CH_3OH	CH_2O	C_2H_5OH	2-C_3H_7OH	cyclobutanol[b]	THF
s1	8.3E+05	8.3E+05	8.3E+05	8.3E+05	8.3E+05	8.3E+05
s2	4.3E+04	4.3E+04	4.3E+04	4.3E+04	4.3E+04	4.3E+04
s3	2.5E−02	2.5E−02	2.5E−02	2.5E−02	2.5E−02	2.5E−02
s4	1.0E+07	1.0E+07	1.0E+07	1.0E+07	1.0E+07	1.0E+07
s5	1.0E+04	1.0E+04	1.0E+04	1.0E+04	1.0E+04	1.0E+04
s6	2.0E+06	2.0E+06	2.0E+06	2.0E+06	2.0E+06	2.0E+06
s7	**5.3E+02**	**4.0E+02**	**2.3E+03**	**1.7E+03**	**2.4E+03**	**7.5E+03**
s8	**6.3E+02**	**1.0E+03**	**1.8D+03**	**3.3D+03**	**4.9D+03**	**2.0E+03**
s9	1.5E+09	1.5E+09	1.5E+09	1.5E+09	1.5E+09	1.5E+09
s10	8.0E+07	1.0E+09	3.8E+08	5.8E+08	4.0E+03	3.8E+08
s11	4.2E+09	4.5E+09	4.6E+09	3.9E+09	3.8E+09	4.6E+09
s12	1.0E+06	1.0E+06	1.0E+06	1.0E+06	1.0E+06	1.0E+06
s13	9.7E+08	8.0E+08	1.9E+09	1.9E+09	1.9E+09	4.0E+09
s14	1.5E+06	1.5E+06	1.5E+06	1.5E+06	1.5E+06	1.5E+06
s15	1.0E+01	1.0E+06	5.0E+01	6.6E+02	0.0E+00	5.0E+01
s16	1.2E+06	1.2E+06	1.2E+06	1.2E+06	1.2E+06	1.2E+06
s17	8.3E+05	8.3E+05	8.3E+05	8.3E+05	8.3E+05	8.3E+05
s18	7.0E+08	1.0E+09	4.0E+08	5.5E+06	1.0E+06	4.0E+08
s19	1.0E+06	1.0E+06	1.0E+06	1.0E+06	1.0E+06	1.0E+06
H_2O_2 calcd[c]	31	31	40	37	40	56
H_2O_2 expt[d]	26,[e] 29[f]	29[f]	33,[e] 34[f]	36,[e] 29[f]	35,[e] 46[f]	49[f]

[a] Units: s^{-1} or $M^{-1}\ s^{-1}$. Data from this work, refs 19,37,43,48, and Notre Dame Radiation Chemistry Data Center compilations, http://www.rcdc.nd.edu/Solnkin1/. Rate constants for one-electron and two-electron reactions of $Fe^{IV}O^{2+}$ are highlighted in bold. [b] Data for *n*-propyl and *n*-butyl radicals. [c] Calculated concentrations (μM) of H_2O_2 generated in reaction. [d] Experimentally found concentrations of H_2O_2. Conditions: 125 μM Fe_{aq}^{2+}, 130 μM O_3, 45−560 mM substrate (see Results), 0.10 M $HClO_4$, 0.4 mM O_2, 25 °C. [e] Titanium oxysulfate method. [f] Initial rate method.

The closeness of the calculated and experimental yields of H_2O_2 was then taken as a measure of the validity of the proposed mechanism. As seen in Table 3, the two sets of data agree to within 20% for all the substrates, a precision that we consider good in view of the large number of reactions.

The simulations of the overall stoichiometry of the Fe_{aq}^{2+}/O_3 reaction in the presence of methanol and ethanol were also carried out. The measured and predicted values agreed to within 5−8%.

Scheme 4 and the calculated branching ratios are further supported by the product data for cyclobutanol. Under the conditions in Figure 3, the NMR yield of cyclobutanone was 129 μM. The simulations predict a reassuringly close value of 113 μM. The difference is believed to be a good measure of the precision one can place on the branching ratios for all the substrates in Table 3.

Qualitatively, most of the substrates examined here have similar branching ratios, with the exception of acetone, acetonitrile, and THF, which clearly prefer the one-electron path. Similar pattern was observed before in the reactions with chromyl ions.[22] Like most other substrates, ethers reacted with $Cr_{aq}O^{2+}$ by a 2-e mechanism, but the reaction was slower than those for other substrates of comparable C−H bond strengths. Reactions with acetone and acetonitrile were too slow to observe.[22]

Now that the reaction scheme has been established, the shape of the k_{obs} vs [S] plots, such as that in Figure 2, can be addressed. The higher slopes at low substrate concentrations have been reported previously for ethanol and formic acid[20] and rationalized by the reaction of $O_2^{\bullet -}$ and $Fe^{IV}O^{2+}$, eq 8−10. The step in eq 10, which doubles the rate of $Fe^{IV}O^{2+}$ consumption, is important only at low substrate concentrations, i.e., when reaction 8 is slow.[20]

(47) Uher, G.; Gilbert, E.; Eberle, S. H. *Vom Wasser* **1991**, *76*, 225−234.
(48) von Sonntag, C. *The chemical basis of radiation biology*; Taylor & Francis: London, 1987; pp 57−92.

$$Fe^{IV}O^{2+} + HCOOH \rightarrow Fe_{aq}^{3+} + CO_2^{\bullet-} + H_2O \quad (8)$$

$$CO_2^{\bullet-} + O_2 \rightarrow CO_2 + O_2^{\bullet-} \quad (9)$$

$$O_2^{\bullet-} + Fe^{IV}O^{2+} \rightarrow \text{products} \quad (10)$$

It is now clear that not only reaction 10 but also other side reactions, especially those consuming or generating Fe_{aq}^{2+}, (Schemes 3 and 4) will also have an impact on the overall stoichiometry and precise kinetics of the disappearance of $Fe^{IV}O^{2+}$ in Fe_{aq}^{2+}/O_3/substrate reactions. The chemistry becomes less complicated at higher substrate concentrations, because $Fe^{IV}O^{2+}$ is exhausted in reaction 8 before the side reactions become important.

Qualitatively, there is a correlation between the observed rate constants for substrate oxidations and C−H bond strengths of the substrates, but the data for acetone and acetonitrile would fall well below the imaginary line through the rest of the data. Such deviations are not unexpected. Acetone and acetonitrile typically react in hydrogen transfer reactions more slowly than alcohols and ethers of comparable C−H bond energies. Rather than plotting the data against a purely thermodynamic parameter, such as the bond energy, it may be more instructive to correlate the data with those for other oxidants with established hydrogen atom transfer mechanisms.[49] As shown in Figure 4, there exists a linear correlation between the reactivities of $Fe^{IV}O^{2+}$ and excited state $*U_{aq}O_2^{2+}$ toward organic substrates.

It may not be obvious why such a correlation should exist, given that one oxidant ($*UO_2^{2+}$) reacts by hydrogen atom transfer, and the other ($Fe^{IV}O^{2+}$), by dual pathways with various proportions of each for different substrates. The answer lies in the specifics of both the chemistry and experimental conditions (excess ozone; see Experimental Section and Table 1) for the $Fe^{IV}O^{2+}$ reactions. The kinetics are dominated by the one-electron path, which removes $Fe^{IV}O^{2+}$ irreversibly. The two-electron, catalytic chemistry does not contribute to the disappearance of $Fe^{IV}O^{2+}$, because the latter is rapidly regenerated from Fe_{aq}^{2+} and excess ozone, making this path kinetically invisible until most of the ozone is consumed. At that time, the concentration of $Fe^{IV}O^{2+}$ has already been severely depleted by the one-electron chemistry. Kinetic traces are largely unaffected by the events taking place in the final stages of the reaction.

Based on the kinetics data alone, previous studies concluded that $Fe^{IV}O^{2+}$ oxidizes alcohols, ethers, and similar substrates exclusively by hydrogen atom abstraction. We have now demonstrated the importance and, in some cases, even dominance of two-electron chemistry that couples Fe(IV) to Fe(II). Such chemistry is essential for iron-based catalysis, as the intermediate 3+ oxidation state cannot be easily reoxidized to Fe(IV). We are currently exploring the effect of reaction conditions, substrates, and other variables on the 1-e/2-e branching.

On the basis of the observed kie's of 4.5 for the oxidation of methanol and 4.6 for 2-propanol, see Table 1, we conclude that the one-electron process probably takes place by hydrogen atom transfer. The two-electron path could involve hydride transfer, as observed previously for $Cr_{aq}O^{2+}$,[22,23] although the data are insufficient for any detailed mechanistic conclusions.

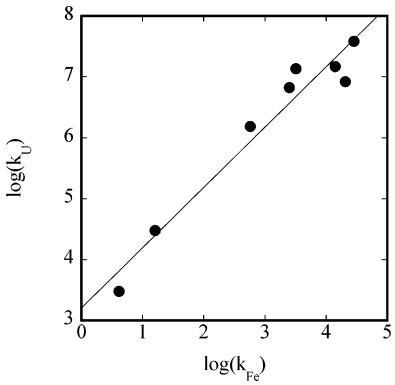

Figure 4. Correlation of the reactivities of $Fe^{IV}O^{2+}$ and excited state $*U_{aq}O_2^{2+}$ toward organic substrates. Second-order rate constants, k_{Fe} and k_U, are given for the following, from left to right: acetonitrile, acetone, methanol, ethanol, 2-propanol, benzyl alcohol, propionaldehyde, and benzaldehyde. Conditions: 0.10 M aqueous $HClO_4$ ($Fe^{IV}O^{2+}$); 0.6 M aqueous H_3PO_4 ($*U_{aq}O_2^{2+}$), 25 °C. Data for $*U_{aq}O_2^{2+}$ from refs 49−51.

Scheme 5

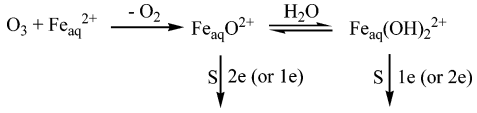

Scheme 6

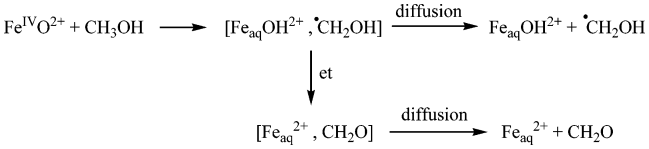

It is certainly possible for hydrogen atom and hydride transfer to take place from the same transition state or intermediate. We are, however, intrigued by the possibility that the source of different products may be the occurrence of slightly different reactions. For example, there may be more than one Fe(IV) species in solution. A rapidly equilibrating mixture of two species, each reacting by one or the other mechanism, could produce the observed results. A simple acid−base equilibrium will not suffice, however, because the yields of Fe_{aq}^{2+} were unaffected by pH. A more realistic possibility is shown in Scheme 5, where the initially formed $Fe_{aq}(O)^{2+}$ undergoes reversible hydration to $Fe_{aq}(OH)_2^{2+}$.

It is also possible that all the oxidations start out as hydrogen atom abstraction reactions forming Fe_{aq}^{3+} and carbon radicals inside the solvent cage. The competition between cage escape and second-electron transfer within the cage, Scheme 6, then determines the ratio of one-electron vs two-electron pathways.

We rule out the possibility that different products arise from the reactions at more than one site in the substrate, as is known to happen with OH radicals.[52] $Fe^{IV}O^{2+}$ reacts much more slowly than $HO^{\bullet}$ and is expected to discriminate among various kinds of C−H bonds. An additional argument against the attack at more than one site is found in the oxidation of methanol, which has only one kind of C−H bonds, yet both pathways operate.

Finally, the assumed 2+ charge[20] for $Fe^{IV}O^{2+}$ has been confirmed in this study by conductivity measurements. The most

(49) Wang, W.-D.; Bakac, A.; Espenson, J. H. *Inorg. Chem.* **1995**, *34*, 6034−6039.
(50) Mao, Y.; Bakac, A. *J. Phys. Chem.* **1996**, *100*, 4219−4223.
(51) Wang, W.-D.; Bakac, A. Unpublished results.
(52) Buxton, G. V.; Greenstock, C. L.; Helman, W. P.; Ross, A. B. *J. Phys. Chem. Ref. Data* **1988**, *17*, 513−886.
(53) Thompson, R. C. *Inorg. Chem.* **1986**, *25*, 184−188.

obvious species consistent with this charge are $Fe^{IV}O^{2+}$, $Fe^{IV}(OH)_2^{2+}$, or a mixture of the two. The reported pK_a of 2.0[20] would appear to tip the scale toward the dihydroxo form in equilibrium with the trihydroxo species, but the definite assignment will have to await more spectroscopic data.

Acknowledgment. We are grateful to Dr. Alan Queen of Tritech Dynamic Instruments for his expertise and persistence in designing, testing, and improving several generations of the conductivity stopped-flow. This manuscript has been authored by Iowa State University under Contract No. W-7405-ENG-82 with the U.S. Department of Energy.

Supporting Information Available: Examples of kinetic data and results of the global fit analysis. This material is available free of charge via the Internet at http://pubs.acs.org.

JA0457112